Discrete Load-Modulated Single-RF MIMO Transmitters

Mohammad A. Sedaghat*, Ralf R. Müller*†, Georg Fischer*, Arslan Ali*

* Friedrich-Alexander Universität Erlangen-Nürnberg, Erlangen, Germany
† Norwegian University of Science and Technology, Trondheim, Norway

***Abstract*—Some recent progresses in Load-Modulated Single-RF (LMSRF) multiple-antenna transmitters are presented including the circuit analysis in the case of closely spaced antennas. Mutual coupling effect is considered and it is shown that there is no need for any decoupling network since the mutual coupling effect can be considered in digital baseband domain. Furthermore, discrete LMSRF is introduced and an implementation method for it using PIN diodes and microstrip lines is presented. Some simulation results for Orthogonal Frequency Division Multiplexing (OFDM) signals with Quadrature Amplitude Modulation (QAM) and Quadrature Phase Shift Keying (QPSK) inputs are presented, e.g., it is shown that using 8 switches in every load modulator results in a signal to distortion ratio of $17.8\mathrm{dB}$ at the transmitter.**

***Index Terms*—Load modulator, power efficiency, matching network, mutual coupling, RF switch.**

I. Introduction

Multiple-Input Multiple-Output (MIMO) systems are used to enhance the throughput in wireless communication networks. The standard implementation of MIMO transmitters uses one RF-chain including a Digital to Analog Converter (DAC), a power amplifier (PA) and a mixer, per antenna element [1]. In this paper, we call such a scheme as Multi-RF (MRF) MIMO transmitter. MRF has some issues related to the size and the cost of the system as follows:

-*The size issue*: in MRF, to avoid the destructive effect of mutual coupling, the antennas are required to be spaced at least at half a wavelength apart. This leads to a size issue in the MIMO transmitters with large number of antennas. Alternatively, compact MRF transmitters have been proposed, e.g., [2]–[4]. Compact MRF transmitters use multi-port matching networks, e.g., a Multi-port Conjugate Matching (MCM) network [5], [6], to alleviate the mutual coupling effect. Such matching networks are complicated to implement for large number of antennas but feasible for small number of antennas, e.g., the case of 3 antennas in [7].

-*The cost issue*: in MRF, each antenna requires its own RF-chain; therefore, the larger the number of antennas, the higher the cost. Furthermore, due to the frequent use of signals with high Peak-to-Average Power Ratio (PAPR) such as Orthogonal Frequency Division Multiplexing (OFDM) in modern wireless communication systems, linear power amplifiers with high back-off are required. This reduces power efficiency and increases the cost of the system further. Hardware efforts to improve the efficiency of power amplifiers include dynamic biasing [8], dynamic supply modulation [9], [10] and dynamic load modulation [11]. Another option is to use PAPR reduction techniques [12].

A single-RF multi-antenna transmitter called Electronically Steerable Passive Array Radiator (ESPAR) has been proposed in [13] for analog beamforming and in [14] for MIMO systems. ESPAR allows for a compact implementation in hand-held devices [15]. ESPAR is suitable for a transmitter with small number of antennas. The tunable load connected to each passive antenna is purely imaginary to avoid Ohmic losses. Thus, only limited types of modulations can be supported e.g., PSK modulation as presented in [15]. Note that recently ESPAR with arbitrary loads has been also proposed which requires more complicated load circuits [16].

Load-Modulated Single-RF (LMSRF) MIMO transmitters have been proposed in [17], [18] to reduce the RF-cost and also enable compact arrays in MIMO communications. Circuit and power efficiency analyses in the case of no mutual coupling effect are given in [17]. In this paper, we consider the case of LMSRF with compact arrays and introduce a new structure for LMSRF which has some advantages compared to one introduced in [17]. The analysis in the case of compact arrays is given and it is shown that mutual coupling effect can be considered in the digital basedband domain without extra effort in the RF domain. Next, we introduce an implementation method for load modulators using PIN diodes and microstrip lines. The simulation results of the proposed circuit are presented.

The new architecture of LMSRF is presented in Section II. The analysis for compact arrays is given in Section III. Section IV describes a new implementation method for load modulators including some simulation results. Finally, Section V concludes the paper.

II. LMSRF architecture

In an LMSRF transmitter, there is only one source which is a Local Oscillator (LO) followed by a PA as shown in Fig. 1. The constant envelope sinusoid signal passes through a two-port matching network. This matching network matches the star point, shown by v_s in Fig. 1, to the PA. Each antenna element is connected to the star point via a load modulator

This work was supported in part by the European FP7 project HARP (High capacity network architecture with remote radio heads & parasitic antenna arrays) under grant agreement no. 318489.

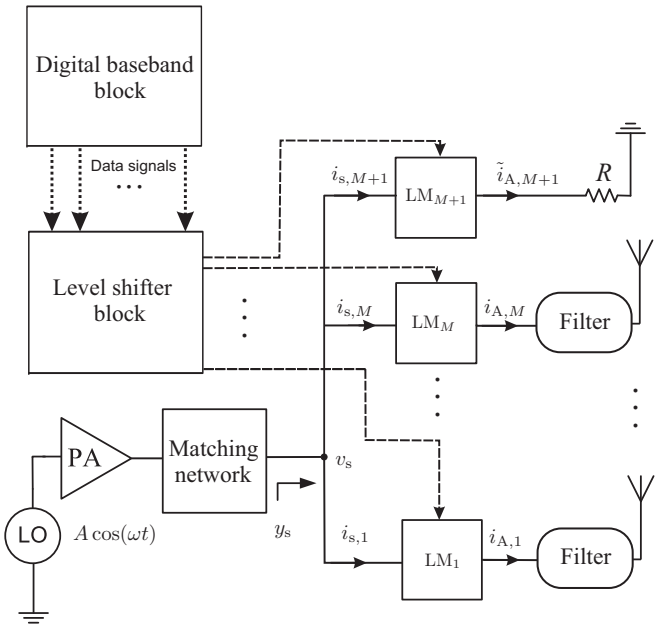

Fig. 1. The architecture of LMSRF MIMO transmitter.

(shown by LM_m in Fig. 1). A load modulator is a two-port network which contains some tunable components, e.g., diodes, to control the current on each antenna.

All the digital baseband processing steps such as source coding, mapping, channel coding, precoding, are done at the baseband block. The output signals of the baseband block are some digital commands to the level shifter block. The level shifter produces the required bias voltages for the tunable components in the load modulator blocks (see Fig. 1). The processing rate is equal to the symbol rate.

It is assumed that all the transmission lines in Fig. 1 are lossless and multiples of half a wavelength long. The structure shown in Fig. 1 has an extra load modulator (shown by LM_{M+1}) compared to the structure presented in [17]. This extra load modulator is called the Auxiliary Load Modulator (ALM). The ALM is added to the LMSRF to burn the reflected power from the other load modulators.

The PA amplifies a constant envelope signal, thus it requires no back-off and can be non-linear and very efficient. In order to avoid damaging the PA by reflected signals, the input admittance at the star point, i.e, y_s, should be constant and matched to the PA. In other words, although the input admittance of each load modulator changes, the sum admittance of all load modulators should be constant. This ensures that the maximum transfer power condition is met at the output of the PA. In [17], the reflected power is dissipated in a resistance connected to a circulator at the output of the PA; therefore, the voltage at the star point is not constant exactly. However, in the structure shown in Fig. 1, the voltage at the star point is approximately constant. This makes tuning of load modulator blocks much easier. Note that the number of states (which relates to the number of switches) in the ALM determines the amount of reflected power to the PA.

Let P_a and P_r be the output power of the PA and the instantaneous total radiated power, respectively. The extra power $P_R = P_\mathrm{a} - P_\mathrm{r}$ is dissipated as heat in the resistance R. The role of this resistance is to burn the extra power in order to avoid reflection to the PA. The current of the resistance R is controlled by the ALM block.

An analog spectral shaping filter is used to limit the spectral bandwidth on each antenna. The impulse response of the filters may change due to environmental changes. This may cause some errors at the receiver. However, the filters can be considered as part of the channel. As an example, in massive MIMO systems with Time Division Duplex (TDD) mode, the channel is estimated by uplink pilot symbols [19]. The same filters are also used in the receive mode to limit the noise bandwidth. Due to the reciprocity of the channel, the impulse responses of the filters can be estimated as parts of the channel.

A. Discrete load modulation using RF switches

Load modulator blocks can be implemented using switches, e.g., MEMS switches or PIN diodes, called Discrete Load Modulator (DLM) or using soft tunable components, e.g., varactor diodes, called Soft Load Modulator (SLM).

Let's assume a modulation scheme with N constellation points on the antennas. In DLM, there are some finite states. The baseband block determines the $\log_2(N)$ bits for each antenna and then based on these bits, the level shifter serves the voltage signals to switch to the desired constellation point for each antenna at every symbol time.

In SLM, there are some continuous tunable elements which are capable of changing the impedance seen from one of its ports in a continuous manner tuning the bias conditions. In this scheme, the exact value of bias voltage is generated using some DACs . SLM suffers from non-linearity problem of tunable components, low speed and power handling problems [20]. DLM offers high speed switching using PIN diodes without requiring any DAC. In this paper, we propose to use DLM to avoid the non-linearity problem.

DLM can be implemented using some Π or T networks serially connected [21]. In DLM, variable capacitors are implemented by connecting some switches serially to some capacitors. Thus, different states for the currents on the antennas can be obtained by changing the states of the switches. Six-port modulators are another way of implementing DLM [22], [23], which are appropriate for higher frequency ranges due to the size constraint. In this paper, we propose another way of implementing DLM using distributed transmission lines.

III. Analysis for compact antenna arrays

In this section, we show that LMSRF MIMO transmitters allow for compact arrays without degrading the performance and requiring complicated matching networks. In the analysis, complex voltage and current envelopes are considered as port variables. Let $\boldsymbol{Z}_\mathrm{A}$ be the impedance matrix of the antennas connected to the filters. The radiated power in this case is calculated as

$$P_\mathrm{r} = \boldsymbol{i}_\mathrm{A}^\dagger \Re\{\boldsymbol{Z}_\mathrm{A}\}\boldsymbol{i}_\mathrm{A}, \tag{1}$$

where $\boldsymbol{i}_A$ is the current vector after the load modulators (excluding the ALM) as shown in Fig. 1. Note that the current of the resistance R is calculated using the power equation

$$P_{\rm a} - P_{\rm r} = R|i_R|^2. \tag{2}$$

Assuming a standard MIMO receiver and using the multi-port model described in [24], the received vector can be modeled as

$$\boldsymbol{y} = \boldsymbol{Z}_{\rm TR}\boldsymbol{i}_{\rm A} + \boldsymbol{n}, \tag{3}$$

where $\boldsymbol{Z}_{\rm TR}$ is the transfer matrix between the received vector and the currents on the transmit antennas and $\boldsymbol{n}$ is the additive white Gaussian noise at the receive antennas. To obtain a consistent channel model with the standard MIMO model [24], we set $\boldsymbol{i}_{\rm A} = \Re\{\boldsymbol{Z}_{\rm A}\}^{-\frac{1}{2}}\boldsymbol{x}$, where $\boldsymbol{x}$ is considered as the input vector. Thus, the total radiated power becomes

$$P_r = \boldsymbol{x}^{\dagger}\boldsymbol{x}, \tag{4}$$

and the channel model is

$$\boldsymbol{y} = \underbrace{\boldsymbol{Z}_{\rm TR}\Re\{\boldsymbol{Z}_{\rm A}\}^{-\frac{1}{2}}}_{\boldsymbol{H}}\boldsymbol{x} + \boldsymbol{n}. \tag{5}$$

It is assumed that the coupling matrix $\boldsymbol{Z}_{\rm A}$ is known at the transmitter.

We use admittance model to describe the circuit shown in Fig. 1. In order to design the load modulator blocks, we first set the input admittance at the star point, $y_{\rm s}$, arbitrarily. Let's assume that the output port of the PA is modeled by a Thevenin equivalent with the parameters $v_{\rm a}$ and $z_{\rm a}$. Let's also assume that the matching network is a lossless reciprocal network with the following admittance matrix

$$\boldsymbol{Y}_{\rm c} = \begin{bmatrix} jy_{\rm c11} & jy_{\rm c12} \\ jy_{\rm c12} & jy_{\rm c22} \end{bmatrix}, \tag{6}$$

and mth load modulator has a admittance matrix

$$\boldsymbol{Y}_m = \begin{bmatrix} jy_{m,11} & jy_{m,12} \\ jy_{m,12} & jy_{m,22} \end{bmatrix}. \tag{7}$$

Note that in (6) and (7), we use $y_{\rm c12} = y_{\rm c21}$ and $y_{m,12} = y_{m,21}$, respectively, since the matching network and the load modulators are reciprocal. Then, having $y_{\rm s}$, the admittance parameters of the matching network are designed to satisfy

$$y_{\rm a}^* = jy_{\rm c11} + \frac{y_{\rm c12}^2}{y_{\rm s} + jy_{\rm c22}}, \tag{8}$$

where $y_{\rm a} = 1/z_{\rm a}$ and $y_{\rm a}^*$ is the complex conjugate of $y_{\rm a}$. Next, applying the conjugate matching condition, the voltage at the star point is calculated as

$$v_{\rm s} = v_{\rm a}\frac{jy_{\rm c12}z_{\rm a} - 2jy_{\rm c12}\Re\{z_{\rm a}\}}{2\Re\{z_{\rm a}\}(y_{\rm s} + jy_{\rm c22})}. \tag{9}$$

Let's define the following diagonal matrices

$$\boldsymbol{Y}_{11} = j\mathrm{diag}\left(y_{1,11}, \cdots, y_{M,11}, y_{M+1,11}\right), \tag{10}$$

$$\boldsymbol{Y}_{12} = j\mathrm{diag}\left(y_{1,12}, \cdots, y_{M,12}, y_{M+1,12}\right), \tag{11}$$

$$\boldsymbol{Y}_{22} = j\mathrm{diag}\left(y_{1,22}, \cdots, y_{M,22}, , y_{M+1,22}\right). \tag{12}$$

Then, for the load modulator blocks we have

$$\begin{bmatrix} \boldsymbol{i}_{\rm s} \\ -\tilde{\boldsymbol{i}}_{\rm A} \end{bmatrix} = \begin{bmatrix} \boldsymbol{Y}_{11} & \boldsymbol{Y}_{12} \\ \boldsymbol{Y}_{12} & \boldsymbol{Y}_{22} \end{bmatrix}\begin{bmatrix} \boldsymbol{v}_{\rm s} \\ \boldsymbol{v}_{\rm A} \end{bmatrix}, \tag{13}$$

where $\boldsymbol{i}_{\rm s}$ and $\boldsymbol{v}_{\rm s}$ are the current and voltage vectors at the input ports of the load modulators (including the ALM) as shown in Fig. 1. Moreover, $\tilde{\boldsymbol{i}}_{\rm A}$ and $\boldsymbol{v}_{\rm A}$ are the current and voltage vectors at the output of the load modulators (including the ALM). Let's define

$$\boldsymbol{Y}_{\rm A} = \begin{bmatrix} \boldsymbol{Z}_{\rm A} & \boldsymbol{0}_{M\times 1} \\ \boldsymbol{0}_{1\times M} & R \end{bmatrix}^{-1}. \tag{14}$$

Then, the current at the output ports of the load modulators can be calculated as

$$\tilde{\boldsymbol{i}}_{\rm A} = \boldsymbol{Y}_{\rm A}\boldsymbol{v}_{\rm A}. \tag{15}$$

Let $\boldsymbol{Y}_{\rm s}$ be the input admittance matrix of the load modulators. Substituting (15) in (13) results in

$$\boldsymbol{Y}_{\rm s} = \boldsymbol{Y}_{11} - \boldsymbol{Y}_{12}(\boldsymbol{Y}_{\rm A} + \boldsymbol{Y}_{22})^{-1}\boldsymbol{Y}_{12}. \tag{16}$$

All the input ports of the load modulator blocks are connected to the star point, thus it can be shown that

$$y_{\rm s} = [1, 1, \cdots, 1]\boldsymbol{Y}_{\rm s}[1, 1, \cdots, 1]^{\rm T}. \tag{17}$$

At this point the crucial benefit of LMSRF MIMO transmitters becomes obvious. In order to match the star point to the PA, it is only required to fulfill the scalar conjugate matching constraint as shown in (8) and (17). In compact MRF transmitters, in order to match the antennas to the sources, it is required to have a diagonal $\boldsymbol{Y}_{\rm s}$. This needs a complex decoupling circuit.

From (13) and (15), we have

$$\tilde{\boldsymbol{i}}_{\rm A} = -\boldsymbol{Y}_{\rm A}(\boldsymbol{Y}_{\rm A} + \boldsymbol{Y}_{22})^{-1}\boldsymbol{Y}_{12}v_{\rm s}[1, 1, \cdots, 1]^{\rm T}. \tag{18}$$

In (18), $\tilde{\boldsymbol{i}}_{\rm A}$ and $v_{\rm s}$ are known; therefore, $3(M+1)$ variables of the load modulator blocks can be found numerically using the $2(M+1)$ real equations in (18), one complex equation in (17) and a real equation in (2). Note that the number of variables is more than the number of equations; hence, there are some degrees of freedom to choose the variables.

The result in this section shows that although in LMSRF with compact arrays, the impedance matrix of the antennas is not diagonal, there is no need to decouple the antennas. It is only required to keep $y_{\rm s}$ fixed and match the power amplifier to the star point. In the case of no mutual coupling effect, the vector equation in (18) becomes $M+1$ scalar equations which can be solved independently.

IV. DLM IMPLEMENTATION

In this section, we design DLM using microstrip line and PIN diodes and simulate an LMSRF MIMO transmitter using Advance Design System (ADS) software. We assume that the antennas are far from each other and have a fixed impedance in the considered frequency range. The carrier frequency is 3GHz and the symbol rate is 1Msymbol/s. We use an RF switch shown in Fig. 2 which consists of two PIN diodes,

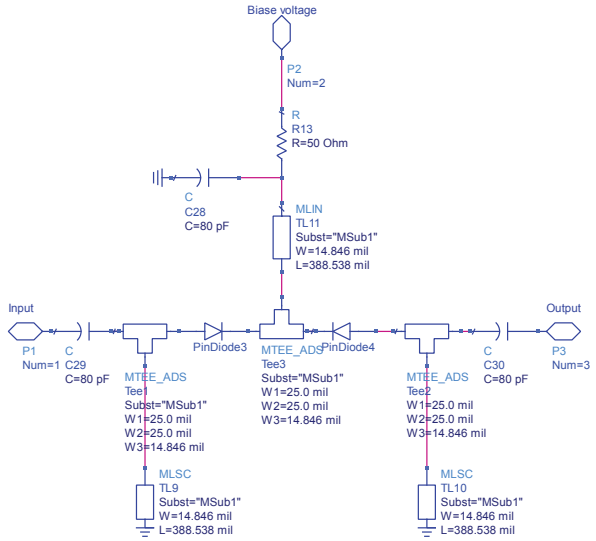

Fig. 2. The switch configuration with two series PIN diodes.

two DC blocker capacitors, and some $\lambda/4$ microstrip lines. In Fig. 2, we use a substrate with the following parameters

- Substrate thickness $\mathrm{H} = 15.24\mathrm{mil}$
- Relative dielectric constant $\mathrm{Er} = 9.6$
- Conductor conductivity in Siemens/meter $\mathrm{Cond} = 10^7$
- Conductor thickness $\mathrm{T} = 0.005\mathrm{mm}$
- Dielectric loss tangent $\mathrm{TanD} = 0.0002$

Furthermore, two PIN diodes with the following parameters are used

- Junction capacitance $= 1\mathrm{fF}$
- Carrier lifetime $\tau = 50\mathrm{ns}$
- I-region width $= 100\mu\mathrm{m}$

Some ± 5-volt DC sources are used to bias the PIN diodes.

The simulation results for the considered switch are plotted in Fig. 3-6. Fig. 3 and Fig. 4 show S_{11} and S_{21} versus frequency when the switch is closed. Next, Fig. 5 and 6 show S_{11} and S_{21} versus frequency, respectively, when the switch is open. The results show that in $f = 3\mathrm{GHz}$, the isolation is about $46\mathrm{dB}$ and the insertion loss is about $0.04\mathrm{dB}$.

Next, we test the switching speed. Fig. 7 and Fig. 8 show the transient output voltage versus time when the switch opens and closes, respectively. It is observed that forward to reverse switching time is the bottleneck of the switch. The switching can be done at about $80\mathrm{Mswitch/sec}$.

Then, we use the structure shown in Fig. 9 for the load modulators. In Fig. 9, the switches change the length of the open stubs. The parameters $l_1, \cdots, l_{13}$ (this is an example for the case of 4 witches) are designed to obtain the output currents with the best covering of the complex space. In the case of m switches in each DLM, 2^m constellation points in the complex space are obtained. Every input symbol is quantized to the closest constellation point. The better the constellation covering, the less the signal distortion.

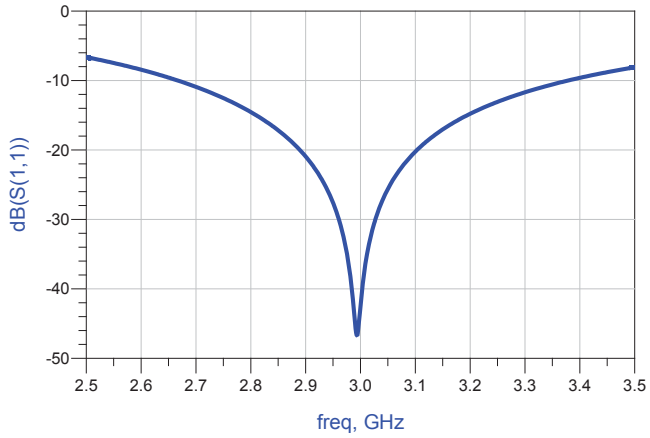

Fig. 3. S_{11} versus frequency when the switch is closed.

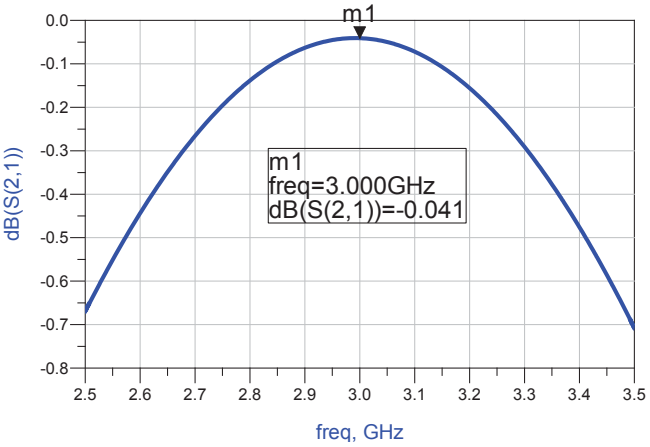

Fig. 4. S_{21} versus frequency when the switch is closed.

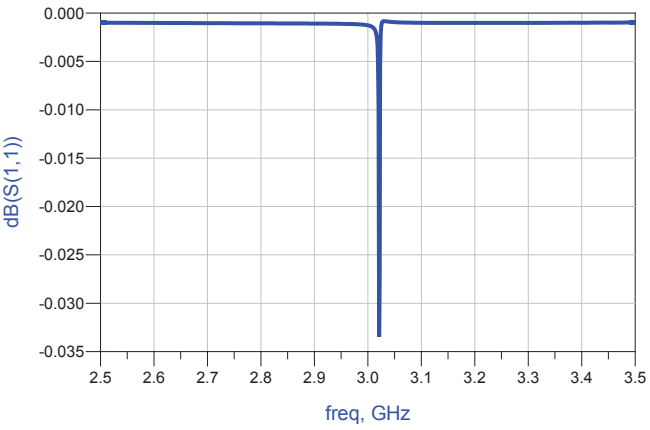

Fig. 5. S_{11} versus frequency when the switch is open.

The goal of the design algorithm is to find the best length for each line in Fig. 9. The problem is a nonlinear and non-convex

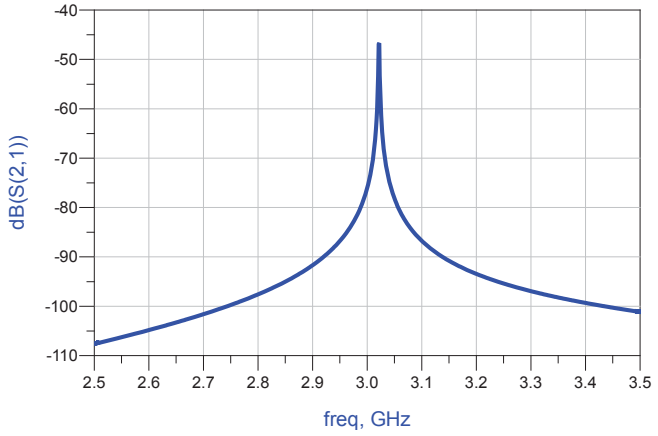

Fig. 6. S_{21} versus frequency when the switch is open.

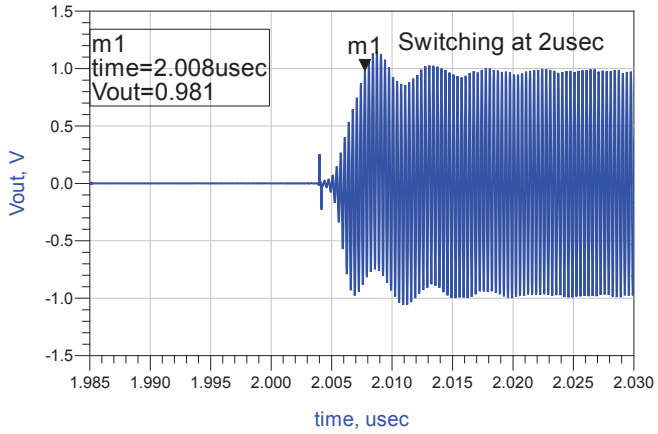

Fig. 7. Reverse to forward switching transient time.

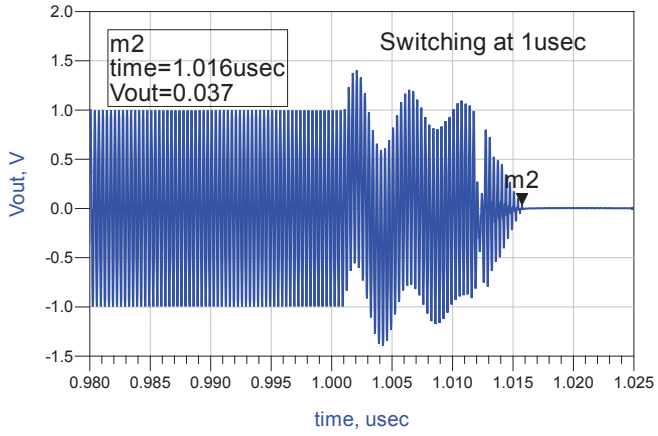

Fig. 8. Forward to reverse switching transient time.

problem. We first use ideal transmission line theory to design avoid complexity and finally we convert the lines to microstrip

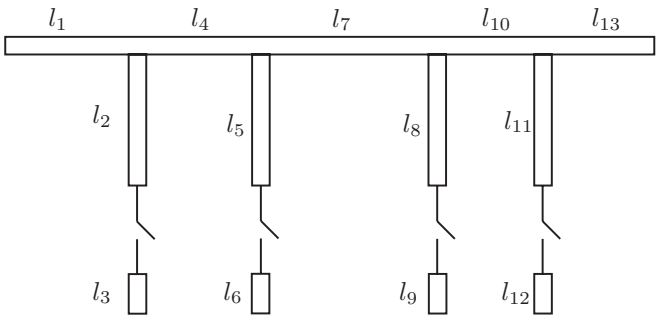

Fig. 9. Load modulator implemented using distributed transmission lines and some switches.

lines. We use Genetic algorithm to find an appropriate solution. We start from a random initial condition. Then, in each iteration of the algorithm, we first generate all the possible output points at the antennas. Then we consider a predefined modulation, e.g., OFDM with 16-QAM input. We generate 10^5 constellation points in digital domain using random input bits. Then, we quantize the constellation points using the possible points at the antennas. This results some error at the output signals. We use the Euclidean distance measure to calculate the error. Note that we limit the line length by using the constraint $\lambda/10 < l_i < \lambda/2$ for implementation purpose. Genetic algorithm converges after many iterations and gives the solution for the length of the stubs.

Fig. 10 shows the resulted output current on one of the antennas in the complex plane for 8 switches in each DLM after using Genetic algorithm. The results are obtained using ADS software and microstrip implementation of the lines in Fig. 9. The resulted points in Fig. 10 shows a good coverage on the complex plane. The transmitter works in the following way: first in the digital baseband block, each output signal is mapped to one of these constellation points. Then, the corresponding switch states are selected to achieve the desired output signals. This means that the output signal on each antenna is quantized by the LMSRF.

The results for signal to distortion ratio versus the number of switches for different signals compared to the theoretical result obtained by Linde-Buzo-Gray (LBG) vector quantization algorithm, are shown in Fig. 11. OFDM with 16-Quadrature Amplitude Modulation (16-QAM) and Quartature Phase Shift Keying (QPSK) are considered. The figure shows about 2dB loss compared to the LBG result when the number of switches is 8.

To connect the antenna branches together we have a problem and that is the variation of voltage and impedance at the star point (the star point is shown by v_s in Fig. 1). This variation means that if we change the state of one of the DLMs, the current on the other antennas are affected as well. To solve this problem, an auxiliary tunable impedance is connected to the star point in order to fix the voltage at the star point. In fact this auxiliary tunable impedance fixes the impedance at the star point. The auxiliary tunable impedance is itself a DLM connected to a resistance as shown in Fig. 1 and called ALM.

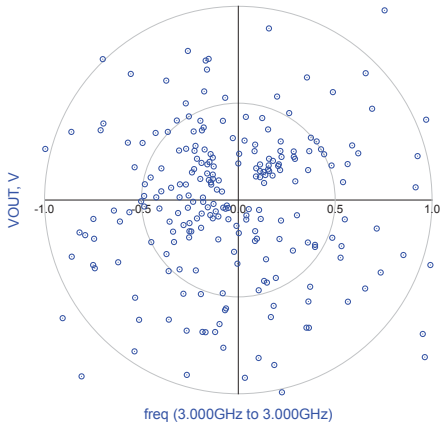

Fig. 10. The resulted constellation for one load modulator with 8 open stubs and 8 switches.

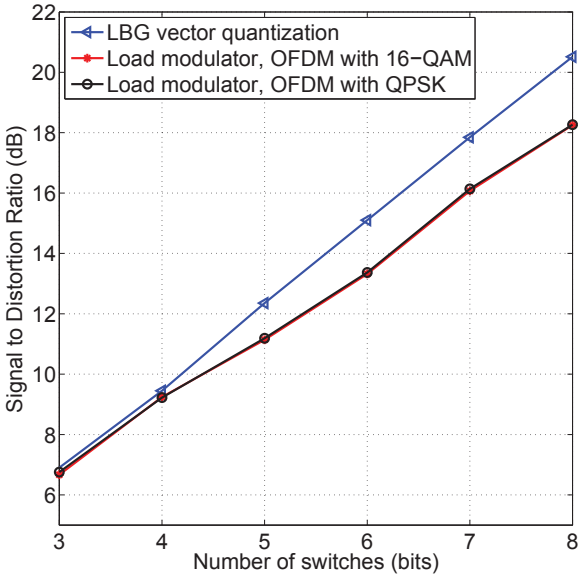

Fig. 11. Signal to distortion ratio versus the number of switches in one load modulator.

Due to the low precision of the ALM connected to the star point, the constellation points move a little as will be shown in the following simulation results. We use the designed LM in a circuit with 10 antennas and an auxiliary LM. We consider QPSK-OFDM and 16-QAM-OFDM constellations. Fig. 12 shows signal to distortion ratio versus the number of bits in the auxiliary LM for 6 and 8 switches in the LMs connected to the antennas.

Fig. 13 and 14 show the constellation points of QPSK and 16-QAM for 8 switches in the LMs connected to the antennas and 6 switches in the ALM. In this case, the signal to distortion ratio is about -17.8dB.

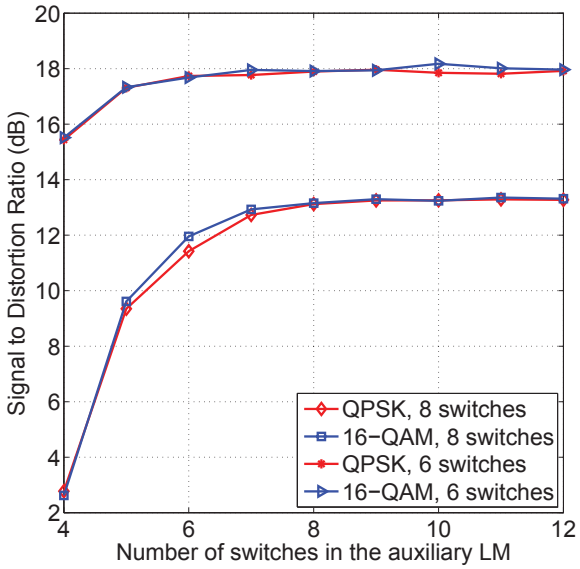

Fig. 12. The signal to distortion ratio versus the number of switches in the auxiliary LM for OFDM modulation with QPSK and 16-QAM symbols.

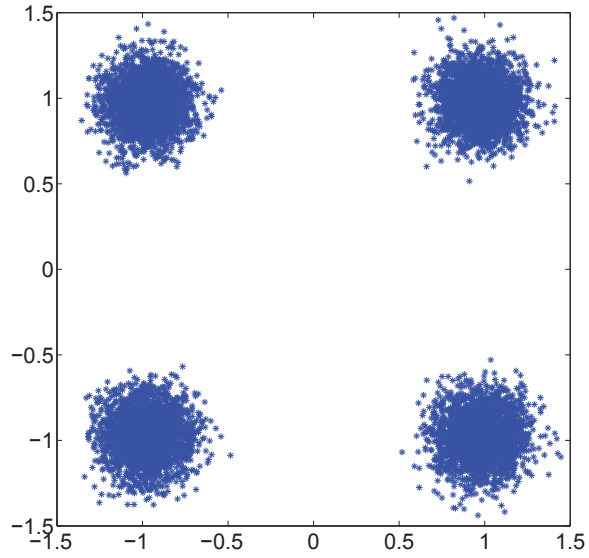

Fig. 13. The resulted constellation of QPSK for 8 switches in the LMs connected to the antennas and 6 switches in the auxiliary LM.

V. Conclusion and Future Works

Some new results in single-RF multi-antenna transmitters were presented. The analysis in the case of compact arrays was given. It was shown that the mutual coupling effect can be considered in baseband digital domain and there is no need for antenna decoupling. An implementation method using PIN diodes and microstrip lines was presented and some simulation results were given.

In this paper, we considered a narrow-band impedance

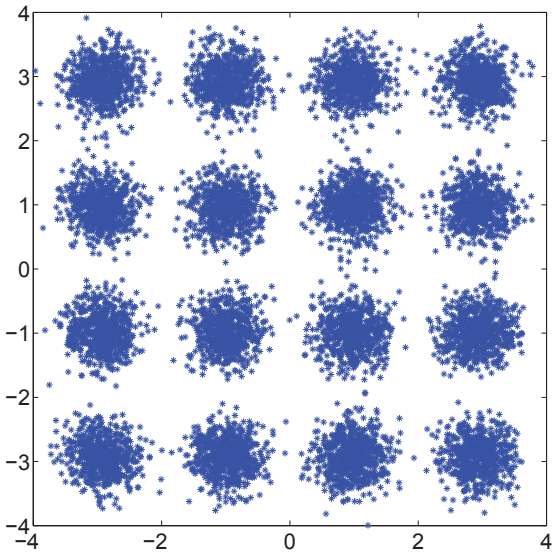

Fig. 14. The resulted constellation of 16-QAM for 8 switches in the LMs connected to the antennas and 6 switches in the auxiliary LM.

model which is fine for small bandwidth signals but not appropriate for large bandwidth signals. As the first future work, one can analyze LMSRF using more precise model. Furthermore, during the analysis, we assumed that the filters and the antennas have fixed impedance behavior in the frequency band. However, for signals with large bandwidth, this is not completely true.

Another question is about the out of band radiation. Since the DLMs switch between some discrete states, there is out of band radiation. The pass-band filters are supposed to cut the out of band radiation but making such sharp filters is not straightforward. One can analyze the system including the effect of the filters.

Nonlinear behavior of DLMs in the switching time period affects the star point voltage and creates some reflected waves to the central PA. Analyzing the precise behavior of the star point is another worthy future work.

REFERENCES

[1] A. Kalis, A. G. Kanatas, and C. B. Papadias, *Parasitic Antenna Arrays for Wireless MIMO Systems*. Springer, 2014.

[2] R. A. Bhatti, S. Yi, and S.-O. Park, "Compact antenna array with port decoupling for LTE-standardized mobile phones," *Antennas and Wireless Propagation Letters, IEEE*, vol. 8, pp. 1430–1433, 2009.

[3] D. W. Browne, M. Manteghi, M. P. Fitz, and Y. Rahmat-Samii, "Experiments with compact antenna arrays for MIMO radio communications," *Antennas and Propagation, IEEE Transactions on*, vol. 54, no. 11, pp. 3239–3250, 2006.

[4] C.-Y. Chiu and R. D. Murch, "Compact four-port antenna suitable for portable MIMO devices," *Antennas and Wireless Propagation Letters, IEEE*, vol. 7, pp. 142–144, 2008.

[5] J. W. Wallace and M. A. Jensen, "Mutual coupling in MIMO wireless systems: A rigorous network theory analysis," *Wireless Communications, IEEE Transactions on*, vol. 3, no. 4, pp. 1317–1325, 2004.

[6] M. T. Ivrlač and J. A. Nossek, "A multiport theory of communications," in *Proceedings of International ITG Conference on Source and Channel Coding*, Siegen, Germany, Jan. 2010.

[7] J. Weber, C. Volmer, K. Blau, R. Stephan, and M. A. Hein, "Miniaturized antenna arrays using decoupling networks with realistic elements," *Microwave Theory and Techniques, IEEE Transactions on*, vol. 54, no. 6, pp. 2733–2740, 2006.

[8] K. Yang, G. I. Haddad, and J. R. East, "High-efficiency class-A power amplifiers with a dual-bias-control scheme," *Microwave Theory and Techniques, IEEE Transactions on*, vol. 47, no. 8, pp. 1426–1432, 1999.

[9] B. Sahu and G. A. Rincon-Mora, "A high-efficiency linear RF power amplifier with a power-tracking dynamically adaptive buck-boost supply," *Microwave Theory and Techniques, IEEE Transactions on*, vol. 52, no. 1, pp. 112–120, 2004.

[10] F. Wang, A. H. Yang, D. F. Kimball, L. E. Larson, and P. M. Asbeck, "Design of wide-bandwidth envelope-tracking power amplifiers for OFDM applications," *Microwave Theory and Techniques, IEEE Transactions on*, vol. 53, no. 4, pp. 1244–1255, 2005.

[11] F. H. Raab, "High-efficiency linear amplification by dynamic load modulation," in *Microwave Symposium Digest, 2003 IEEE MTT-S International*, vol. 3. IEEE, 2003, pp. 1717–1720.

[12] Y. Rahmatallah and S. Mohan, "Peak-to-average power ratio reduction in OFDM systems: A survey and taxonomy," *Communications Surveys & Tutorials, IEEE*, vol. 15, no. 4, pp. 1567–1592, 2013.

[13] T. Ohira and K. Gyoda, "Electronically steerable passive array radiator antennas for low-cost analog adaptive beamforming," in *Phased Array Systems and Technology, 2000. Proceedings. 2000 IEEE International Conference on*. IEEE, 2000, pp. 101–104.

[14] A. Kalis, A. G. Kanatas, and C. B. Papadias, "A novel approach to MIMO transmission using a single RF front end," *IEEE Journal on Selected Areas in Communications*, vol. 26, no. 6, pp. 972–980, Aug. 2008.

[15] O. Alrabadi, C. Papadias, A. Kalis, and R. Prasad, "A universal encoding scheme for MIMO transmission using a single active element for PSK modulation schemes," *IEEE Transactions on Wireless Communications*, vol. 8, no. 10, pp. 5133 –5142, Oct. 2009.

[16] B. Han, V. Barousis, C. B. Papadias, A. Kalis, R. Prasad *et al.*, "MIMO over ESPAR with 16-QAM modulation," *Wireless Communications Letters, IEEE*, vol. 2, no. 6, pp. 687–690, 2013.

[17] M. A. Sedaghat, R. R. Mueller, and G. Fischer, "A novel single-RF transmitter for massive MIMO," in *18th International ITG Workshop on Smart Antennas (WSA)*. Erlangen, Germany: VDE, Mar. 2014.

[18] R. R. Müller, M. A. Sedaghat, and G. Fischer, "Load modulated massive MIMO," in *IEEE GlobalSIP, Massive MIMO Symposiumum*, Atlanta, GA, Dec. 2014.

[19] T. L. Marzetta, "Noncooperative cellular wireless with unlimited numbers of base station antennas," *IEEE Transactions on Wireless Communications*, vol. 9, no. 11, pp. 3590–3600, Nov. 2010.

[20] K. Buisman, C. Huang, A. Akhnoukh, M. Marchetti, L. de Vreede, L. Larson, and L. Nanver, "Varactor topologies for RF adaptivity with improved power handling and linearity," in *Microwave Symposium, 2007. IEEE/MTT-S International*. IEEE, 2007, pp. 319–322.

[21] C. Sánchez-Pérez, J. de Mingo, P. L. Carro, and P. García-Dúcar, "Design and applications of a 300–800 MHz tunable matching network," *Emerging and Selected Topics in Circuits and Systems, IEEE Journal on*, vol. 3, no. 4, pp. 531–540, 2013.

[22] J. Osth, M. Karlsson, A. Serban, S. Gong *et al.*, "Schottky diode as high-speed variable impedance load in six-port modulators," in *Ultra-Wideband (ICUWB), 2011 IEEE International Conference on*. IEEE, 2011, pp. 68–71.

[23] J. Osth, M. Karlsson, A. Serban, and S. Gong, "M-QAM six-port modulator using only binary baseband data, electrical or optical," *Microwave Theory and Techniques, IEEE Transactions on*, vol. 61, no. 6, pp. 2506–2513, 2013.

[24] M. Ivrlac and and J. Nossek, "Toward a circuit theory of communication," *Circuits and Systems I: Regular Papers, IEEE Transactions on*, vol. 57, no. 7, pp. 1663 –1683, Jul. 2010.